Virology 448 (2014) 303–313

Contents lists available at ScienceDirect

Virology

journal homepage: www.elsevier.com/locate/yviro

Enhanced IRES activity by the 3′UTR element determines the virulence of FMDV isolates

Soledad García-Nuñez [a], María Inés Gismondi [a], Guido König [a], Analía Berinstein [a], Oscar Taboga [a], Elizabeth Rieder [b], Encarnación Martínez-Salas [c], Elisa Carrillo [a,*]

[a] Instituto de Biotecnología, Centro de Investigación en Ciencias Veterinarias y Agronómicas, Instituto Nacional de Tecnología Agropecuaria, CC25 B1712WAA Castelar, Buenos Aires, Argentina
[b] Foreign Animal Disease Research Unit, United States Department of Agriculture, Agricultural Research Service, Plum Island Animal Disease Center, PO Box 848, Greenport, NY11944-0848, USA
[c] Centro de Biología Molecular Severo Ochoa, Consejo Superior de Investigaciones Científicas, Universidad Autónoma de Madrid, Cantoblanco, 28049 Madrid, Spain

ARTICLE INFO

Article history:
Received 12 August 2013
Returned to author for revisions
6 September 2013
Accepted 18 October 2013

Keywords:
FMDV
IRES
hSHAPE
RNA structure
3′UTR
Virulence
Infectious cDNA clone

ABSTRACT

A reverse genetics approach was used to identify viral genetic determinants of the differential virulence displayed by two field foot-and-mouth disease virus (FMDV) strains (A/Arg/00 and A/Arg/01) isolated in Argentina during the 2000–2001 epidemics. A molecular clone of A/Arg/01 strain and viral chimeras containing the S-fragment or the internal ribosome entry site (IRES) of A/Arg/00 in the A/Arg/01 backbone were constructed and characterized. The IRES appeared as a determining factor of the lower level of A/Arg/00 replication in cell culture. High-throughput RNA probing revealed structural differences between both IRESs. Translation experiments using either synthetic viral RNAs (*in vitro*) or bicistronic plasmids (*in vivo*) showed that these IRESs' activities differ when the viral 3′ untranslated region (UTR) is present, suggesting that their function is differentially modulated by this region. This work provides experimental evidence supporting the role of the IRES-3′UTR modulation in determining the level of FMDV replication in field strains.

Introduction

Foot-and-mouth disease virus (FMDV) is the prototype member of the Aphthovirus genus in the family Picornaviridae. FMDV produces a highly contagious disease in domestic and wild cloven-hoofed animal species worldwide generating severe economic losses (Sobrino and Domingo, 2004).

The infectious virion is a nonenveloped icosahedron composed of 60 copies of each of the four structural proteins (1A, 1B, 1C and 1D). The viral genome is a single-stranded, positive-sense RNA of about 8400 bases (Jackson et al., 2003; Rueckert and Wimmer, 1984) and is organized in a single open reading frame (ORF) flanked by highly structured 5′ and 3′ untranslated regions (5′UTR and 3′UTR, respectively) (Grubman and Baxt, 2004). After infection of a cell, FMDV RNA is rapidly translated within the cytosol into a single polyprotein which is processed into 14 mature virus proteins, along with several protein intermediates needed for viral replication (Rueckert, 2001). The first element of the 5′UTR is known as the S-fragment, consisting of a long stem-loop that is presumably involved in genome replication and stability. Downstream of a poly(C) tract and a pseudoknots region (Carrillo et al., 2005; Mason et al., 2003), there is a *cis*-active replicative element (cre) that consists of a highly conserved stem-loop known to be essential for FMDV genome replication (Mason et al., 2002). A type II internal ribosome entry site (IRES) constitutes the last element of the 5′UTR and is responsible for initiating the cap-independent translation of the viral RNA (Kuhn et al., 1990). The FMDV IRES contains four structural domains that interact with cellular translation initiation factors and participate in RNA–RNA interactions (Martínez-Salas, 2008; Ramos and Martínez-Salas, 1999). Among these domains, the central domain (known as domain 3) is critical for IRES activity (López de Quinto and Martínez-Salas, 1997). The first region of the ORF encodes the L^{pro} proteinase, known to participate in the polyprotein processing and in the shutoff of host cap-dependent translation (López de Quinto and Martínez-Salas,

* Correspondence to: Elisa Carrillo, Instituto de Biotecnología, Centro de Investigación en Ciencias Veterinarias y Agronómicas, Instituto Nacional de Tecnología Agropecuaria, CC25 B1712WAA Castelar, Buenos Aires, Argentina. Tel.: +54 11 4621 1447; fax: +54 11 4621 0199.
E-mail addresses: mgnunez@cnia.inta.gov.ar (S. García-Nuñez), mgismondi@cnia.inta.gov.ar (M.I. Gismondi), gkonig@cnia.inta.gov.ar (G. König), aberinstein@cnia.inta.gov.ar (A. Berinstein), otaboga@cnia.inta.gov.ar (O. Taboga), elizabeth.rieder@ars.usda.gov (E. Rieder), emartinez@cbm.uam.es (E. Martínez-Salas), ecarrillo@cnia.inta.gov.ar (E. Carrillo).

0042-6822/$ - see front matter © 2013 Elsevier Inc. All rights reserved.
http://dx.doi.org/10.1016/j.virol.2013.10.027

2000; Medina et al., 1993). Cleavage of L^{pro} from the nascent protein chain is followed by processing of P1-2A, P2BC and P3 regions. P1-2A region yields the structural proteins 1A, 1B, 1C and 1D and the non-structural protein 2A, while processing of P2BC and P3 produces the viral non-structural proteins 2B, 2C, 3A, $3B_{1-3}$, $3C^{pro}$ and $3D^{pol}$. Proteins 2A and $3C^{pro}$ mediate the polyprotein processing together with L^{pro}. 2B and 2C, and their precursor 2BC, are implicated in disturbing the structure of membranes in host cells and, along with 3A, participate in viral replication (Moffat et al., 2005; O'Donnell et al., 2001). Three copies of the small viral protein 3B (VPg) are encoded in the FMDV genome. All VPgs can be used but only one of the different forms is attached to any individual RNA priming viral RNA synthesis (Falk et al., 1992; Sangar et al., 1977) by the viral $3D^{pol}$ RNA-dependent RNA polymerase (Lowe and Brown, 1981). The 3′UTR is composed by a sequence of about 90 nucleotides predicted to be structured in two stem-loops followed by a poly(A) tail of variable length (Serrano et al., 2006). This region is essential for FMDV infectivity and replication (Saiz et al., 2001) and presents a stimulatory effect on IRES-dependent translation, even in the absence of a poly (A) tail (López de Quinto et al., 2002).

Although there is plenty of knowledge about the basic aspects of the molecular biology of FMDV, the functional roles of the FMDV protein precursors, mature viral proteins and non-coding sequences in viral replication have not yet been completely elucidated.

FMDV occurs as seven distinct serotypes (A, O, C, SAT-1, SAT-2, SAT-3 and Asia 1) and multiple subtypes, reflecting a wide range of genetic and antigenic variability. Serotypes A and O are distributed worldwide, and they are the only ones reported in South America, along with serotype C (Knowles and Samuel, 2003). In the field, FMDV heterogeneity is reflected by the lack of cross-protection even between intra-serotype variants. At the same time, functional and structural constraints affect the genome mutation rate, constituting an important factor of purifying selection (Domingo et al., 2003).

The FMDV strains A/Argentina/2000 (A/Arg/00) and A/Argentina/2001 (A/Arg/01) were isolated from infected bovines during the 2000–2001 FMDV epidemics that occurred in Argentina. These viruses belong to different phylogenetic lineages and, interestingly, while A/Arg/00 was said to produce mild lesions in the affected animals, strain A/Arg/01 caused severe lesions in cattle in the field as well as in experimental challenge trials (Mattion et al., 2004). In a previous work, our group demonstrated that A/Arg/00 displays lower infectivity in mice than A/Arg/01 and grows less efficiently in cell culture when evaluated in terms of viral particle production. However, viral RNA (vRNA) synthesis was not affected in A/Arg/00, suggesting that other events during the viral cycle would be responsible for the differences in viral growth (García-Nuñez et al., 2010).

In this work, a reverse genetics approach was used to identify defined viral genetic determinants responsible for the different biological characteristics of FMDVs A/Arg/00 and A/Arg/01.

Results

Genome analysis of the FMDV strains A/Arg/00 and A/Arg/01

It has been previously shown that the two FMDV isolates A/Arg/00 and A/Arg/01 differ from each other in terms of their growth characteristics in cell culture and their specific infectivity in suckling mice (García-Nuñez et al., 2010). In this work, the term *virulence* is used to describe the effect of viral replication in cell culture while the term *pathogenicity* refers to the damage caused by viral infection in animals.

To identify the genetic characteristics that might be relevant to determine the differential behavior of these viruses we analyzed their whole-genome sequences (GenBank accession no. AY593782 and AY593786, respectively).

The pairwise comparison revealed multiple nucleotide and amino acid differences all along the genome (Fig. 1 and Fig. S1 in supplementary material). These differences are located in variable positions within FMDV genome. Moreover, to our knowledge, none of these positions have been related so far to FMDV virulence and pathogenicity (Carrillo et al., 2005). As a consequence, the genomic comparison did not allow the identification of critical positions that could be related to phenotypic differences.

It is well documented that the RNA structure of the 5′ and 3′ UTRs is essential for certain viral functions (Martínez-Salas and Ryan, 2010). Therefore, we analyzed through an *in silico* approach whether the nucleotide differences could determine alterations in the secondary structure of the elements that conform these regions. The S-fragment and the IRES element presented differences in their predicted conformation. While secondary structure analysis of the S-fragments predicted a single stem-loop for A/Arg/01, similar to that previously proposed for FMDV (Clarke et al., 1987; Escarmís et al., 1992), the S-fragment of A/Arg/00 folded into an alternative structure with similar free energy levels (Fig. S2A in supplementary material). As expected, the IRES region of FMDVs A/Arg/00 and A/Arg/01 (IRES-00 and IRES-01, respectively) showed predicted secondary structures corresponding to IRES type 2 (Fig. S2C) (Belsham, 2009). However, local structural differences were detected on domain 3; indeed, loops 3c and 3d, along with bulge 3e, did not appear in the predicted structural conformation of IRES-00 (Fig. S2C [I]). When the optimal folding pattern was restricted to nt 839–850 (loop 3c), we observed that, while loop 3c of IRES-01 was predicted to be conserved ($\Delta G = -2.5$ kcal/mol), this structure was not predicted in IRES-00 ($\Delta G = 0.0$ kcal/mol). Conversely, when the optimal folding pattern was restricted to nt 859–875 (loop 3d) the same conformation was observed for both IRES elements ($\Delta G = -5.0$ kcal/mol) (Fig. S2C [II]). On the other hand, no structural differences were observed in cre and 3′UTR (Fig. S2B and S2D).

These findings encouraged us to investigate whether structural differences within the S-fragment and/or the IRES element of FMDV strains A/Arg/00 and A/Arg/01 could explain, at least partly, the differences in virulence between these isolates.

Rescue and characterization of an infectious clone and chimeric derivatives

A reverse genetics approach was utilized to evaluate the putative effect of the S-fragment and the IRES element on viral replication of our particular strains.

First, a cDNA encoding the entire genome of the FMDV A/Arg/01 strain was assembled in plasmid pA2001c (Fig. 2A) that was used to synthesize infectious viral RNA *in vitro*. The infectious virus vA2001c was rescued after transfection of the synthesized transcripts into BHK-21 cell monolayers. Presence of the genetic marker *Nhe*I was confirmed by RT-PCR of the supernatant of transfected cells (Fig. 2A) and sequence analysis demonstrated that the recovered virus derived from the infectious full-length RNA transcript.

Using pA2001c as a backbone, two chimeric plasmids were assembled by substitution of the S-fragment or the IRES with the sequences of the corresponding region of FMDV A/Arg/00. These constructs were named Q-S.00 and Q-IRES.00, respectively. The viral chimeras were obtained by transfection of the transcripts, synthesized from each linearized plasmid, into BHK-21 cell monolayers.

The phenotypic characteristics of the rescued viruses vA2001c, Q-S.00 and Q-IRES.00 were analyzed in BHK-21 cells and compared with the wild type FMDVs A/Arg/00 and A/Arg/01. As can be seen in Fig. 2B, all the viruses analyzed displayed plaques of clear

morphology. As expected, the plaque sizes of vA2001c (5.2 ± 1.5 mm) did not differ from the plaques produced by FMDV A/Arg/01 (5.4 ± 2.1 mm, $p > 0.05$). Moreover, Q-S.00 plaques (4.5 ± 1.9 mm) were undistinguishable from those produced by A/Arg/01 and vA2001c ($p > 0.05$). Interestingly, Q-IRES.00 presented a small plaque phenotype (1.6 ± 0.7 mm), very similar to FMDV A/Arg/00 (1.5 ± 0.7 mm, $p > 0.05$) and significantly smaller than FMDV A/Arg/01 or vA2001c ($p < 0.001$).

Consistently, the replacement of the FMDV A/Arg/01 IRES (IRES-01) by its counterpart in FMDV A/Arg/00 (IRES-00) negatively affected vA2001c viral yield (Fig. 2C). At 4 hpi, the viral titers produced in cells infected with Q-IRES.00 ($1 \times 10^2 \pm 2.87 \times 10^1$ UFP/ml) were significantly lower than those produced in A/Arg/01, vA2001c or Q-S.00 infected cells ($1.95 \times 10^4 \pm 4.24 \times 10^3$ UFP/ml, $4.25 \times 10^4 \pm 3.53 \times 10^3$ UFP/ml and $2.5 \times 10^4 \pm 7.07 \times 10^3$ UFP/ml, respectively). Notably, Q-IRES.00 titers were not significantly different from FMDV A/Arg/00 titers ($3.00 \times 10^2 \pm 2.82 \times 10^2$ UFP/ml) while Q-S.00 titers did not differ from those produced by A/Arg/01 or vA2001c.

These results show that, while the exchange of the S-fragment does not affect the infectivity of vA2001c, the exchange of the IRES region negatively impacts on it.

Growth kinetics of chimeric virus Q-IRES.00

The results described above led us to characterize more extensively the growth kinetics of Q-IRES.00. To this end, BHK-21 cells were infected at an MOI of 5 with Q-IRES.00, vA2001c, and the FMDVs A/Arg/01 and A/Arg/00. Then, at different times post infection the intracellular viral titers were assessed.

Viruses containing the IRES-00 (A/Arg/00 and Q-IRES.00) presented identical one-step growth curves (Fig. 3A). These viruses grew slower and yielded lower titers than the viruses containing the IRES-01 (A/Arg/01 and vA2001c), consistently with their smaller plaque size and lower titers at 4 hpi. Nevertheless, no significant differences in intracellular vRNA levels were observed in cells infected with FMDVs A/Arg/01, vA2001c or Q-IRES.00 at various times post infection, indicating that the IRES-00 does not affect vRNA accumulation in infected cells (Fig. 3B). Consistently higher levels of vRNA were observed in A/Arg/00 infected cells. In agreement with this and for reasons not clearly understood, previous studies have shown that A/Arg/00 presents a lower ratio of infectivity to intracellular vRNA than A/Arg/01 when evaluated in BHK-21 cells (García-Nuñez et al., 2010).

Next, the kinetics of viral protein synthesis in BHK-21 cells infected with Q-IRES.00 and vA2001c were compared. [^{35}S] methionine was added to infected cells at specific intervals after which the cells were harvested and the radiolabeled viral proteins were immunoprecipitated. As shown in Fig. 3C, different efficiency of viral protein synthesis was observed in cells infected with FMDVs vA2001c or Q-IRES.00. The level of viral protein synthesis in cells infected with vA2001c peaked at 4 hpi, whereas a lower level of viral proteins was detected in Q-IRES.00 infected cells at this time; however, accumulation of viral proteins reached comparable levels at 6 hpi.

Taken together, these results suggest that the IRES region determines the distinguishable characteristics between A/Arg/00 and A/Arg/01 replication in BHK-21 cells.

In vitro translation efficiency of IRES-00 and IRES-01

To further study the effect of IRES-00 on viral translation, *in vitro* analyses were carried out using vA2001c and Q-IRES.00 transcripts (Fig. 4). Equal amounts of viral RNAs were used to program *in vitro* translation reactions. The radiolabeled products were visualized in a 12% SDS-polyacrylamide gel.

The full-length RNA from vA2001c yielded 20% more translational products than the full-length RNA from Q-IRES.00, indicating that IRES-01 promotes vRNA translation more efficiently than IRES-00 within the genomic context.

Overall, the results presented so far suggest that IRES-00 is a determining factor of the lower level of viral replication exhibited by the FMDV A/Arg/00.

Structural analysis of IRES-00 and IRES-01

The spatial conformation of the IRES region is crucial for its biological function as it allows the recognition by RNA-binding proteins and the RNA-mediated regulation of internal initiation of translation (Martínez-Salas, 2008).

To gain insight into the molecular basis of infectivity differences between FMDVs A/Arg/00 and A/Arg/01, the secondary structure of the IRES elements was analyzed by hSHAPE, using *in vitro* synthesized transcripts of IRES-00 and IRES-01, along with NMIA as the modifying agent (McGinnis et al., 2009).

Overall, hSHAPE reactive nucleotides of both IRES elements were located within RNA structures predicted to be single stranded (Fig. 5), in agreement with *in silico* prediction results. However, IRES-00 secondary structure as determined by hSHAPE differed from the predicted structure, particularly in domains 2 and 3 (compare Fig. 5 and S2C in supplementary material), thus reflecting the necessity of including experimental information in RNA prediction algorithms.

Both IRES elements presented differences in the number and degree of reactivity of flexible nucleotides mainly in the apical region of domain 3. The major differences were localized in loops 3b and 3c and, in a lesser extent, within loops 3d and 3e. Additionally, hSHAPE reactivity was also detected within the other IRES domains, where single flexible nucleotides differed between IRES-00 and IRES-01.

Effect of the 3′UTR on IRES-dependent translation

The 3′UTR of the FMDV genome, located between the polymerase coding region and the poly(A) tract, stimulates IRES activity in BHK-21 cells (López de Quinto et al., 2002). Moreover, the FMDV IRES and the 3′UTR interact through strand-specific RNA–RNA contacts when evaluated *in vitro* (Serrano et al., 2006). Therefore, given that there are sequence differences within the 3′UTR of these strains (Fig. S1B), it was of interest to evaluate the role of the 3′UTR as one of the determining factors of differences in IRES-dependent translation. To this end, we first synthesized vA2001c and Q-IRES.00 RNAs from templates in which the 3′UTR and the poly(A) tract were selectively removed using a unique restriction site located immediately upstream of the 3′UTR; then, equal amounts of these vRNAs were used to program *in vitro* translation reactions. Interestingly, unlike what happened when the reactions were programmed with the complete genomes (see Fig. 4), there were no significant differences in the translation efficiency of both vRNAs (Fig. 6A). The band intensity quantification showed similar results in reactions loaded either with vA2001c RNA or with Q-IRES.00 RNA. Taken together, these results suggest that while the efficiency of translation of both FMDV IRESs was comparable, IRES-dependent translation could be differentially stimulated by the presence of 3′UTRs within the viral genomic context.

With the objective of further analyzing the functional activity of both IRES elements we generated CAT/Luc bicistronic constructs in which translation of the Luc reporter gene was driven alternatively by IRES-00 or IRES-01 (pIRES-00/Luc and pIRES-01/Luc, respectively). At the same time, to study the involvement of the 3′ UTR of each virus in the differential modulation of IRES-dependent translation in living cells, the 3′UTR region of FMDV A/Arg/00

(3′.00) or A/Arg/01 (3′.01) was inserted downstream of the Luc stop codon in the bicistronic constructs to generate all the possible combinations (pIRES-00/3′.00, pIRES-00/3′.01, pIRES-01/3′.00 and pIRES-01/3′.01). Then, IRES-dependent translation was quantified in cells transfected with the previously mentioned plasmids through the expression of Luc normalized to that of CAT (cap-dependent translation).

In agreement with *in vitro* experiments, in which viral genomes lacking the 3′UTR presented equal amounts of viral proteins synthesized, the constructs pIRES-00/Luc and pIRES-01/Luc exhibited indistinguishable efficiencies of IRES-dependent translation activity showing that both IRESs are equally able of promoting translation *in vivo* (Fig. 6B). Interestingly, when the 3′UTR previous to the poly (A) tract from FMDVs A/Arg/00 or A/Arg/01 were included in plasmids containing the IRES-01, IRES-dependent translation was stimulated. On the contrary, neither 3′UTR region was capable of generating a significant stimulation of IRES-dependent translation in plasmids containing the IRES-00 ($p > 0.05$). Of note, similar amounts of Luc mRNA were detected by qPCR in transfected cells, suggesting that the differences observed in Luc expression were not mediated by an improved stability of the transcripts (data not shown).

Taken together, these results strongly suggest that the activity of both IRESs is similar and that IRES-01 activity is stimulated by the presence of a 3′UTR located in cis.

Discussion

Factors that control the interaction between any given virus and its host determine the success of infection. Therefore, a better understanding of them is critical for prevention and treatment of viral diseases.

FMDV is genetically and antigenically variable; there is no cross-protection among the seven known serotypes and only

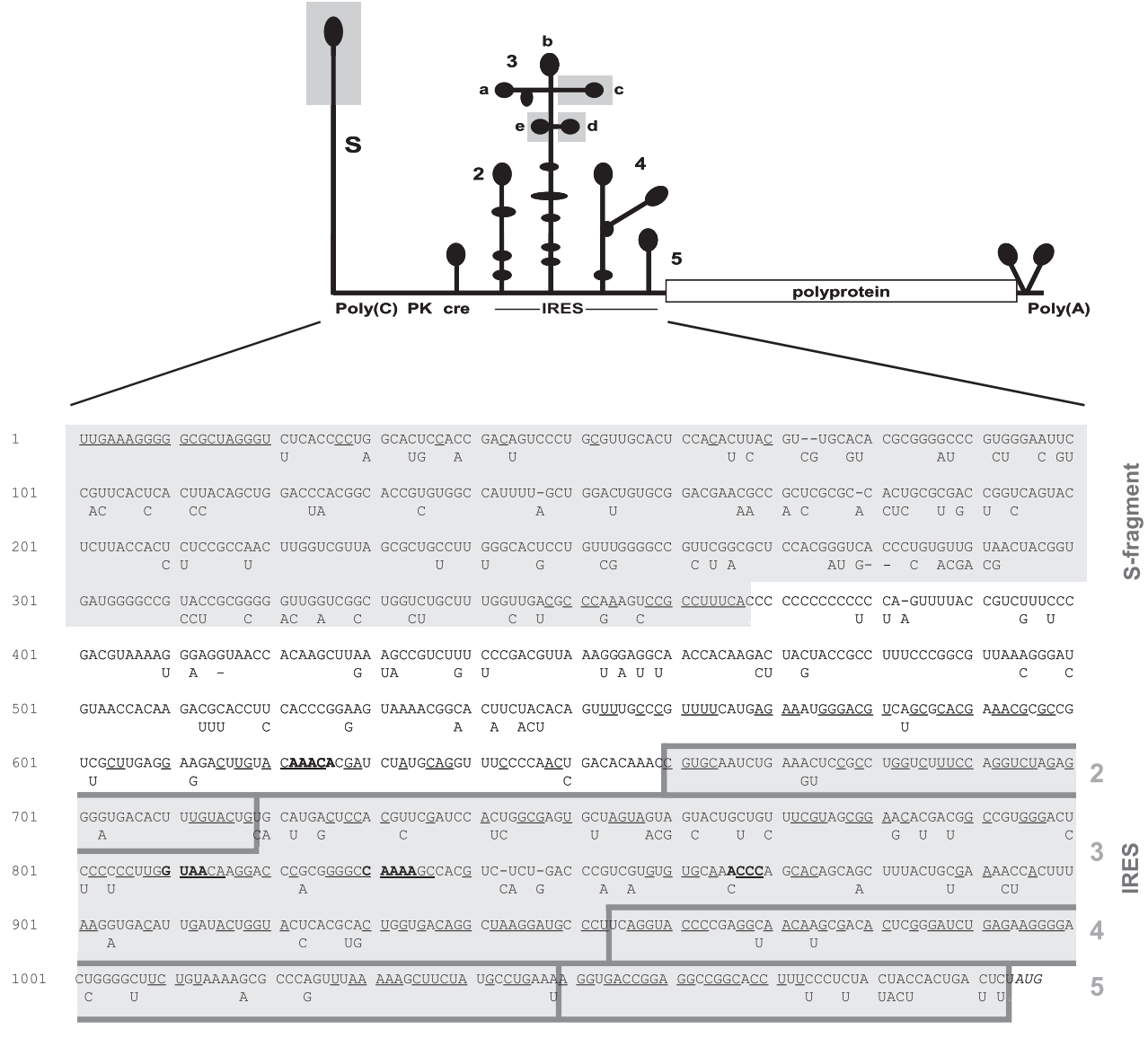

Fig. 1. 5′**UTR sequence comparison of the FMDVs A/Arg/00 and A/Arg/01.** *Top*, schematic representation of the FMDV genome showing the location and secondary structure of the 5′UTR; the grey rectangles depict the regions with predicted secondary structures that differ between both viruses. *Bottom*, 5′UTR sequence of FMDV A/Arg/00 where the nucleotide differences present in A/Arg/01 are shown below the corresponding A/Arg/00 nucleotide; conserved FMDV nucleotides as reported by Carrillo et al. (2005) are underlined; conserved motifs located at the cre (AAACA) and at the IRES domains 3a, 3b and 3d (GNRA, CRAAA and ACCC, respectively) are represented in bold and the first AUG of the polyprotein is shown in *italics*. The sequences corresponding to the S-fragment (nt 1—367) and the IRES element (nt 661—1094) are depicted in grey; the sequences corresponding to IRES domains 2–5 are boxed and indicated on the right.

limited cross-protection exists among the numerous subtypes within a serotype (Martínez et al., 1988). This level of heterogeneity is also reflected in the severity of the disease in the natural hosts which varies with the virus strain (Donaldson, 2004). Recently, we have reported the characterization of two FMDV strains that showed pathogenicity differences in cattle during the 2000–2001 outbreaks that occurred in Argentina.

Hypothetically, as any change in the structural or non-structural proteins or in the viral noncoding RNA elements could impair virus infection, it may also define the degree of viral virulence and/or pathogenicity (Grubman and Baxt, 2004). Thus, it became interesting to further investigate what factors contribute to the biological differences displayed by these two viruses isolated from a natural host. This work provides experimental evidence supporting the role of the IRES-3′UTR cooperation in determining the level of FMDV replication.

Initially, the comparative analysis of A/Arg/00 and A/Arg/01 sequences revealed multiple nucleotide and amino acid changes between the two FMDV strains. Based on published information (Carrillo et al., 2005), we have not been able to directly correlate them with the virulence level. Also, the predicted secondary structure of the RNA elements at the 5′ and 3′ UTRs showed that the S-fragment and the IRES display structural particularities in each virus strain. However, the peculiarities observed between both S-fragments did not affect the virulence of A/Arg/00 and A/Arg/01 since viral populations genetically identical except for the S-fragment showed no differences in the size and morphology of their lysis plaques or in their viral production. On the other hand, further studies are required to elucidate whether the differences in the predicted structure of FMDV A/Arg/00 S-fragment certainly occur within an infected cell.

Through hSHAPE analysis of IRES-00 and IRES-01, diversity in the number and position of reactive nucleotides was identified mainly in the apical region of domain 3, thus demonstrating the existence of conformational differences between these FMDV IRESs. The apical region is a cruciform structure that determines the structural organization of the self-folding domain 3, and has a critical role in IRES activity (Fernández-Miragall and Martínez-Salas, 2003; Fernández et al., 2013, 2011). Disruption of IRES conserved motifs located in the loops 3a, 3b and 3d negatively affects IRES activity and usually provokes a rearrangement of the structural conformation of the apical region (Fernández-Miragall et al., 2006; López de Quinto and Martínez-Salas, 1997). Although no conserved motif has been identified in the loop 3c and in the bulge 3e, these structures seem to be present in every FMDV IRES element (Carrillo et al., 2005). In support of this, structural alterations of the bulge 3e also lead to a local reorganization of the apical region and affect IRES activity (Fernández et al., 2013).

On the other hand, differences observed between *in vitro* and *in vivo* DMS accessibility of the FMDV IRES suggest a distinct RNA conformation in the cellular environment (Fernández-Miragall and Martínez-Salas, 2007). Therefore, further investigation is needed to address whether the nucleotide differences between IRES-00 and IRES-01 determine a different conformational structure *in vivo*.

The IRES element is responsible for internal initiation of translation of viral RNA; this critical function indicates that the IRES could play an important role in viral pathogenicity. In fact, it has been shown that specific mutations in the IRES element of poliovirus are involved in reduced neurocytopathic phenotype (Gromeier et al., 1996), probably as a result of changes in the secondary structure of RNA. In this work, it has been demonstrated that the presence of the IRES-00 in the genome of FMDV A/Arg/01 confers to the virus the phenotypic characteristics of FMDV A/Arg/00. When present in the context of the complete viral genome, the diminished capacity of IRES-00 to synthesize viral proteins indicates a direct involvement of the IRES region for the differences observed between FMDVs A/Arg/00 and A/Arg/01.

The differences in translation efficiency were not observed when Q-IRES.00 and vA2001c derived transcripts lacked the 3′ UTR. Previous studies demonstrated that FMDV RNAs lacking the poly(A) tract and/or the 3′UTR previous to the poly(A) present a reduced efficiency of RNA translation in cell-free extracts and are not infectious when transfected into susceptible cells (López de Quinto et al., 2002; Sáiz et al., 2001). As a consequence, the effect of each IRES within FMDV genomes lacking the 3′UTR on viral replication can only be studied *in vitro*. In agreement with our previous results, when IRES-00 and IRES-01 were included in bicistronic constructs, outside the context of the viral genome, they did not differ in their capacity to drive initiation of protein synthesis. Conversely, when the 3′UTR previous to the poly (A) tract of either virus was included, only the bicistronic construct with the IRES-01 displayed an enhanced activity in BHK-21 cells, suggesting a higher activity of IRES-01 in the presence of a 3′UTR in comparison with IRES-00. Although direct RNA–RNA interactions between the FMDV IRES element and the 3′UTR have been demonstrated *in vitro* (Serrano et al., 2006), the molecular mechanisms of the FMDV IRES-3′UTR interaction that occur within the host are not yet understood.

The lack of significant differences observed when BHK-21 cells were transfected with bicistronic constructs carrying only the IRES-00 or the IRES-01 and no 3′UTR suggests that the direct interaction between each IRES and the cellular factors would not be altered in either virus. However, it cannot be ruled out that some of these cellular factors may be interacting with some other element of the viral genome, thus differently affecting IRES-00 and IRES-01 activities. Indeed, a chimeric virus including the non-structural proteins 2C, 3A, $3B_{1-3}$, 3C, 3D and the 3′UTR of A/Arg/00 in the molecular context of the vA2001c genome showed an intermediate virulence, with intermediate plaque size and viral particle production values (data not shown). Therefore, one or more of the elements included in the substituted region (2C, 3A, $3B_{1-3}$, 3C, 3D and 3′UTR) moderately diminishes vA2001c virulence. Although genome incompatibility could have a role in such phenotypic differences, up to date this event has only been reported among different serotypes (Van Rensburg and Mason, 2002).

In addition, it cannot be ruled out that other elements of the viral genome may have a role in the differential activity of IRES-00 and IRES-01 during viral infection. Consistent with this, it has been demonstrated that poliovirus 2A and FMDV Lb proteases induce an important stimulation of IRES activity and a simultaneous inhibition of the cap-dependent cellular mRNA translation in BHK-21 and in normal rat kidney (NRK) cells (Roberts et al., 1998). Therefore, FMDV Lb protease might also be differently modulating IRES-00 and IRES-01 activities *in vivo*.

IRES mutations have been associated to phenotype differences between field isolates in the picornaviruses Enterovirus 71, Hepatitis A virus and ECHO virus (Gharbi et al., 2006; Li et al., 2011; Mackiewicz et al., 2010). However, no experimental determination of RNA conformation was performed in those works in order to thoroughly assess the alterations in the structure of their IRES elements. In a previous work, we showed that two wild-type FMDV serotype A strains with the same spatio-temporal distribution present different phenotypic characteristics (García-Nuñez et al., 2010). Here, we demonstrate an enhanced IRES-01 activity when the FMDV 3′UTR is present in cis, suggesting that IRES-00 and IRES-01 function is differentially modulated by this genomic region. We propose that these functional differences are based on structural dissimilarities between both IRESs.

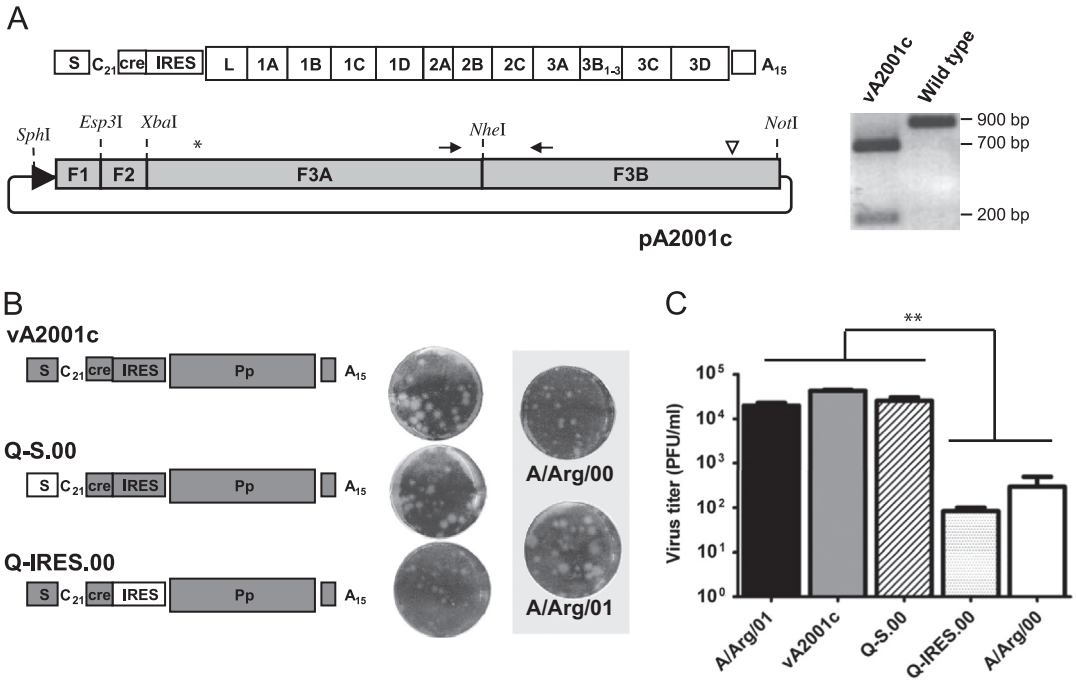

Fig. 2. Construction, rescue and characterization of an infectious cDNA clone of FMDV A/Arg/01 and the chimeric virus derivatives Q-S.00 and Q-IRES.00. (A) *Left*, four overlapping subgenomic fragments were obtained by RT-PCR from A/Arg/01 RNA and cloned. Each plasmid was cut with unique restriction enzymes, which are shown in the figure, and the products were ligated to recover a complete full-length cDNA clone denominated pA2001c. The black arrowhead upstream of the F1 fragment represents a T7 RNA polymerase promoter, the asterisk indicates the *Bst*EII restriction site used to construct the Q-IRES.00 chimera and the white arrowhead indicates a unique *Stu*I restriction site. The *Nhe*I restriction site was engineered as a genetic marker in order to differentiate the infectious clone from the parental virus. Black arrows denote primer annealing sites for RT-PCR mediated amplification of a 900 bp fragment containing the genetic marker *Nhe*I. *Right*, the 900 bp PCR fragment amplified from the supernatant of transfected cells containing vA2001c was incubated with *Nhe*I and visualized in a 1% agarose gel. The supernatant of FMDV A/Arg/01 infected BHK-21 cells (wild type) was used as a positive control of the RT-PCR reaction. (B) *Left*, schematic representation of vA2001c and the constructs Q-S.00 and Q-IRES.00. Grey bars, A/Arg/01; white bars, A/Arg/00; narrow bars represent FMDV non-coding regions and wide bars the FMDV polyprotein (Pp) coding region. *Right*, BHK-21 cells were infected with the different viruses and plaque diameter was measured at 48 hpi as described in *Materials and methods*; the plaque morphologies are shown beside each virus construction and the plaque morphologies of the parental viruses A/Arg/00 and A/Arg/01 are depicted in grey. (C) Monolayers of BHK-21 cells were infected with the indicated viruses at an MOI of 5. Viral yields at 4 hpi were determined in BHK-21 cells by plaque assay and expressed in PFU/ml. Samples were taken in duplicates and standard deviations are shown in the graph. $^{**}p < 0.01$. The results are representative of two independent experiments.

Materials and methods

Cell lines and viruses

Baby hamster kidney cells (BHK-21 clone 13; ATCC CCL10) were maintained in Dulbecco's modified Eagle medium (DMEM, HyClone, Logan, UT, USA) containing 10% fetal bovine serum and supplemented with antibiotics (Gibco-BRL/Invitrogen, Carlsbad, CA, USA).

FMDV A/Arg/00 (prototype strain MC38796 from General Villegas) and FMDV A/Arg/01 (prototype strain MC267 from Trenque Lauquen) were obtained from the National Institute for Animal Health (SENASA, Argentina). These viruses were isolated from infected animals from 2000 to 2001 outbreaks.

All experiments were conducted using second cell passages of each FMDV.

Construction of an infectious cDNA clone of FMDV A/Arg/01 and viral chimeras

FMDV A/Arg/00 and A/Arg/01 RNAs were prepared using the Trizol method (Invitrogen, Carlsbad, CA, USA) and cDNAs were synthesized with SuperScript® III reverse transcriptase (Invitrogen, Carlsbad, CA, USA) as described by the manufacturer. Ninety to 500 ng of total RNA along with 2 picomoles of the antisense oligonucleotide F3Ba (5′–GGCGGCCGCTTTTTTTTTTTTTTTGT-3′) and 50 ng of random hexamers were used for reverse transcription reactions.

In order to construct an infectious cDNA clone of FMDV A/Arg/01, primers were designed as described previously (Rieder et al., 1993). A *Nhe*I genetic marker was engineered into the cDNA clone (Fig. 2A) to distinguish recombinant progeny virus from the parental virus. Four overlapping cDNA fragments were amplified by PCR. Because of its high copying fidelity, Platinum® *Pfx* DNA Polymerase (Invitrogen, Carlsbad, CA, USA) was used, along with 0.5 μM each primer. Typical amplification profiles included 35 cycles of 1 min at 94 °C, 1 min at 55 °C, and 5 min at 68 °C. All PCR-amplified fragments were gel purified and cloned into the pCR 2.1-TOPO vector (Invitrogen, Carlsbad, CA, USA). Positive clones were characterized by restriction endonuclease analysis and sequencing. Cloned fragments were excised with restriction enzymes and finally assembled in a pBacPAK8 vector (Clontech Laboratories Inc., Mountain View, CA, USA). The recombinant plasmid containing the full-length cDNA was named pA2001c.

Chimeric constructs were generated by replacing selected regions of pA2001c by the corresponding regions of FMDV A/Arg/00. In order to do so, two overlapping fragments encompassing the A/Arg/00 *S*-fragment and IRES element were amplified. The generated fragments were cloned using a pCR 2.1-TOPO vector (Invitrogen, Carlsbad, CA, USA) and the plasmids obtained were named pTOPO-S.00 and pTOPO-IRES.00, respectively. pTOPO-S.00 was digested with *Sph*I and *Esp3*I restriction enzymes and the excised 500 bp restriction fragment was used to replace the corresponding fragment of pA2001c to generate pQ-S.00. To obtain a chimeric cDNA that includes the FMDV A/Arg/00 IRES element within the pA2001c backbone, pTOPO-

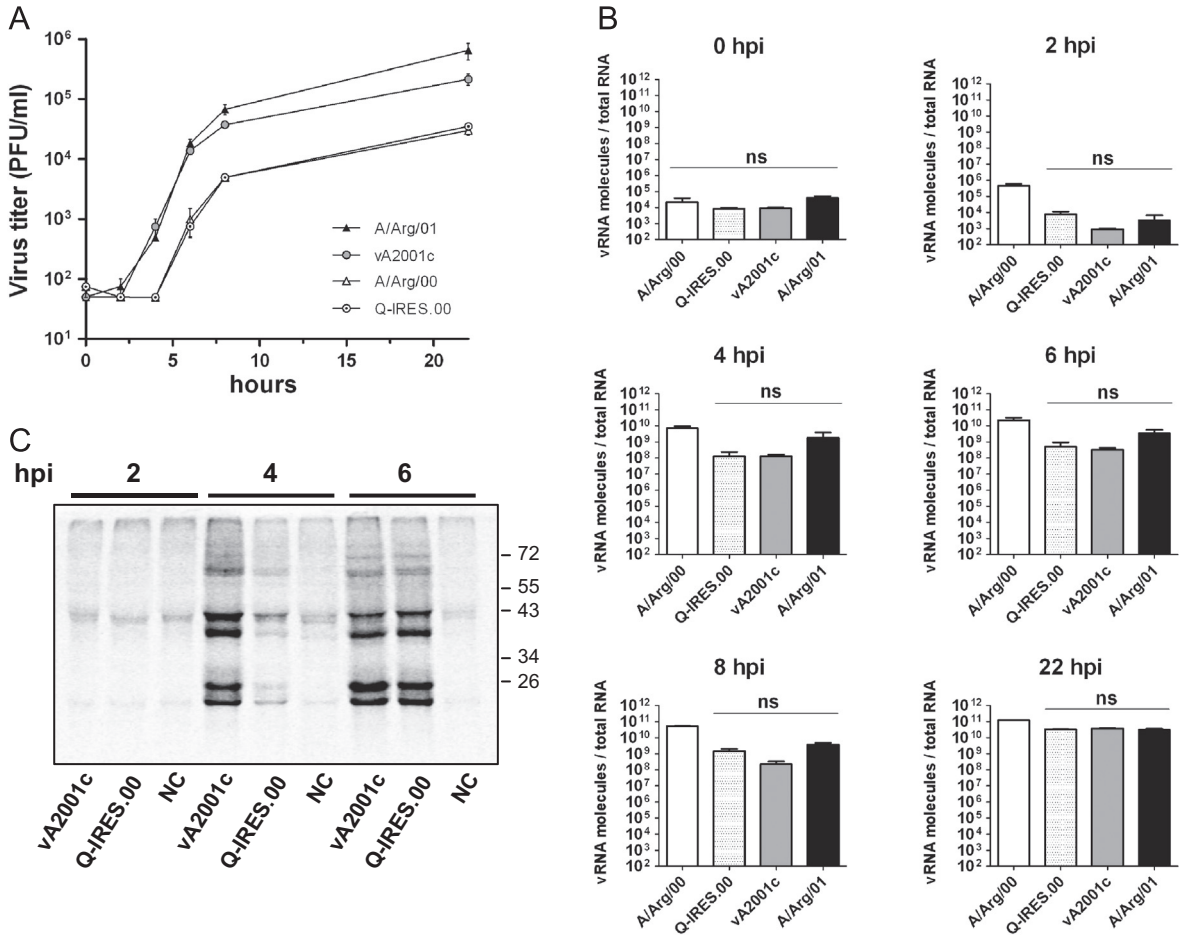

Fig. 3. Growth kinetics of Q-IRES.00. BHK-21 cells were infected with Q-IRES.00, vA2001c and, when indicated, with FMDV A/Arg/00 and A/Arg/01, at an MOI of 5 and harvested at different times post infection. (A) Single-step growth curves were obtained by plaque assay titration of intracellular virus at each time point. Samples were taken in duplicates and standard deviations are shown in the graph. (B) vRNA synthesis as determined by qPCR from Trizol-resuspended monolayers. vRNA was calculated as the number of vRNA molecules relative to nanograms of total extracted RNA (García-Nuñez et al., 2010) ns: not significant. (C) Infected cells were incubated with [^{35}S] methionine for 30 min at 1.5, 3.5 or 5.5 hpi. Equal amounts of radiolabeled protein were immunoprecipitated with guinea pig convalescent serum and aliquots were analyzed by SDS-PAGE on a 12% gel. NC: radiolabeled mock-infected cell extracts.

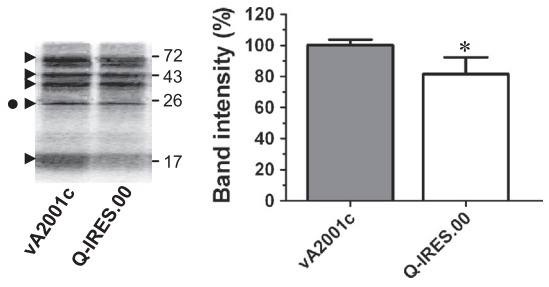

Fig. 4. *In vitro* translation efficiency of Q-IRES.00 transcripts. Synthetic RNAs of ~8.2 kb were obtained from *Not*I linearized plasmids pQ-IRES.00 and pA2001c and were used to program *in vitro* translation reactions in rabbit reticulocyte lysates at 30 °C in the presence of [^{35}S] methionine. *Left,* equal volumes of each *in vitro* translation mix were resolved by 12% SDS-PAGE and fluorography. Arrowheads indicate the bands selected for intensity quantification; the band indicated with the black circle corresponds to 1D. *Right,* band intensity quantification was performed using a phosphorimager and values were relative to vA2001c, which was set at 100%. The results are representative of three experiments and error bars represent standard deviation. *$p < 0.05$.

IRES.00 and pA2001c were digested with *Xba*I and *Bst*EII and the pTOPO-IRES.00-derived 450 bp fragment was inserted in pA2001c generating the construct pQ-IRES.00.

Rescue of virus from full-length cDNA plasmids

The plasmids containing the desired full-length cDNAs were linearized at a *Not*I site located downstream of the poly(A) tract (Fig. 2A). RNAs were synthesized with the MEGAscript T7 kit (Ambion, Austin, TX, USA) according to the manufacturer's specifications and transfected into 80% confluent BHK-21 cells using DMRIE-C reagent (Gibco-BRL/Invitrogen, Carlsbad, CA, USA). After 48 h the cells were freeze-thawed in their growth media and clarified by centrifugation to obtain the initial virus stock in the supernatant. Cells were infected for 24 h between passages. A total of 2 passages after transfection were made for each virus.

To identify the rescued viruses, supernatants were collected and subjected to RNA extraction with Trizol reagent (Invitrogen, Carlsbad, CA, USA) and cDNAs were synthesized as described above. A 900 bp fragment including the genetic marker *Nhe*I was amplified with 0.6 μM of primers 2B1s and A5200a (5′-CGGCCCCCGTCTTCAGTTT-3′ and 5′-ACATTGCCACAGGATTGG-3′, respectively) and 2 U GoTaq DNA Polymerase (Promega, Madison, WI, USA) following manufacturer's instructions. The amplification profile consisted of 35 cycles of 1 min at 94 °C, 1 min at 52 °C and 90 s at 72 °C. To rule out amplification from residual plasmid template, controls consisting of reactions without the addition of RT were performed in parallel. Afterwards, each chimeric region was amplified by PCR as described above and analyzed by automated sequencing.

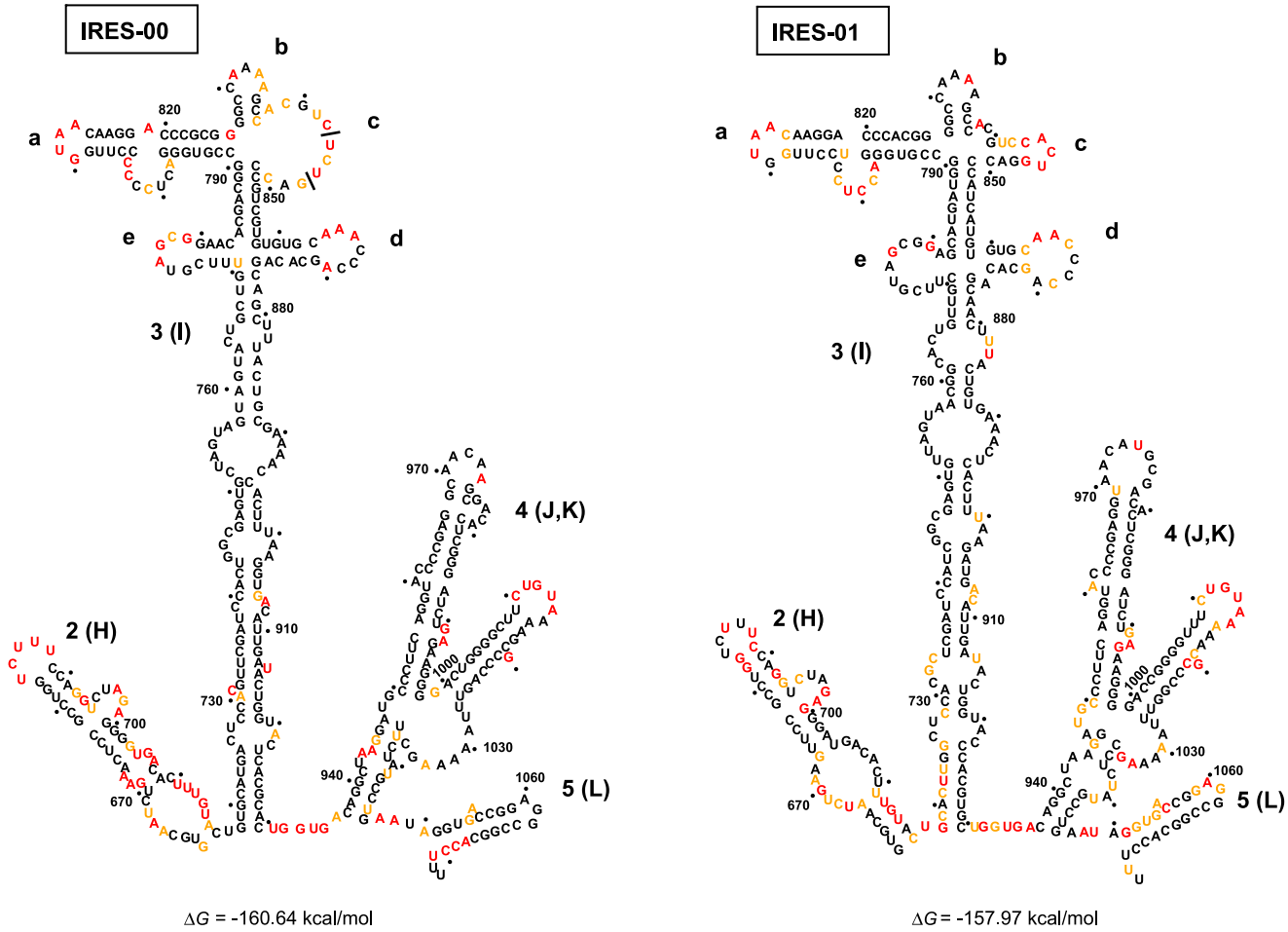

Fig. 5. hSHAPE reactivity of the IRES elements of FMDV A/Arg/00 and A/Arg/01. (A) RNA structure of each FMDV IRES inferred from hSHAPE reactivity. Nucleotides with reactivity ≥ 0.7 are depicted in red and nucleotides with reactivity ≥ 0.3 are depicted in orange. Nucleotide numbering is as in Fig. 1 and a black line between nucleotides indicates a nucleotide deletion in that position. All values correspond to the mean hSHAPE reactivity ($\pm$ SD) of two independent assays.

Plaque assays, viral growth and metabolic labeling

Plaque assays and one-step growth kinetics were performed as previously described (García-Nuñez et al., 2010). Cell monolayers were fixed and stained at 48 h post infection (hpi) and the plaques were counted. The values calculated for the number of plaque forming units per milliliter (PFU/ml) were plotted in a logarithmic scale using GraphPad Prism 5.00 (GraphPad Software, San Diego, CA, USA). All assays were performed in duplicate. For viral plaque size determination, 40 to 60 plaques of each virus were measured with ImageJ 1.42q software (NIH, USA). Data were statistically analyzed by one-way analysis of variance (ANOVA) and Tukey post ANOVA test.

For one step-growth studies, BHK-21 cells were infected for 1 h at an MOI of 5, washed with PBS pH 4 to inactivate unabsorbed virus and incubated at 37 °C. At indicated times post-infection, cells were harvested and virus titers in the clarified supernatants were determined by PFU/ml. When indicated, vRNA synthesis was assayed at each time post-infection as described previously (García-Nuñez et al., 2010).

For metabolic labeling assays, infected BHK-21 cells grown in 25 cm^2 flasks were incubated for 1.5, 3.5 or 5.5 h in culture medium (DMEM, 1% fetal bovine serum). Then, the medium was removed and cells were incubated for 30 min at 37 °C in DMEM without methionine and cysteine (Gibco-BRL/Invitrogen, Carlsbad, CA, USA), but supplemented with [^{35}S] Met–Cys (400 mCi/mmol, Perkin-Elmer, Waltham, MA, USA). Cells were washed twice with ice-cold PBS and collected in 0.2 ml of RSB-NP40 buffer (Tris 10 mM pH7.4, $NaCl_2$ 10 mM, $MgCl_2$ 1.5 mM, NP40 0.01%). Cell extracts were immunoprecipitated with A/Arg/01 guinea pig convalescent sera using Protein A Sepharose (GE Healthcare, Uppsala, Sweden). Immunoprecipitated proteins were analyzed in a 12% SDS-polyacrilamide gel and then visualized in a Typhoon phosphorimager (GE Healthcare, Uppsala, Sweden).

In vitro translation

To obtain full-length transcripts, plasmids pQ-IRES.00 and pA2001c were *Not*I-linearized. To generate transcripts lacking the 3′UTR, plasmids were linearized with *Stu*I, which has its recognition site immediately downstream of the viral coding sequence. Following examination of RNA integrity in agarose gels, 400 ng of each transcript were translated in 10 µl of rabbit reticulocyte lysate (Promega, Madison, WI, USA) in the presence of 10 µCi of [^{35}S]methionine (10 mCi/ml) following manufacturer's instructions. Reaction mixtures were incubated at 30 °C for 1 h. Aliquots of the translation reaction were loaded onto a 12% SDS-polyacrylamide gel. The gels were dried and fluorographed. Quantification of data was performed using a Typhoon phosphorimager and the ImageQuant™ TL software (GE Healthcare, Uppsala, Sweden).

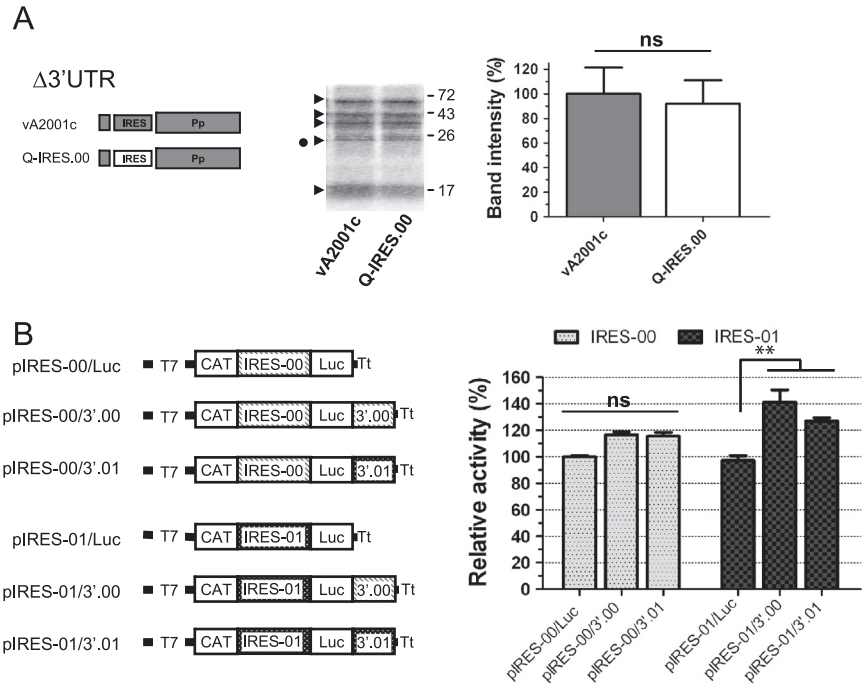

Fig. 6. Influence of the 3′UTR on IRES activity. (A) *Left,* schematic representation of the synthetic FMDV RNAs lacking the 3′UTR that were obtained from *Stu*I linearized plasmids pA2001c and pQ-IRES.00 (see Fig. 2A) and were used to program *in vitro* translation reactions. Grey bars, A/Arg/01; white bars, A/Arg/00; narrow bars represent FMDV non-coding regions and wide bars the FMDV polyprotein (Pp) coding region. *Middle*, equal volumes of each *in vitro* translation mix were resolved by 12% SDS-PAGE and fluorography. Arrowheads indicate the bands selected for intensity quantification; the band indicated with the black circle corresponds to 1D. *Right,* band intensity quantification was performed using a phosphorimager and values were relative to vA2001c, which was set at 100%. Error bars represent standard deviation as calculated from three independent experiments. ns: not significant. (B) Bicistronic constructs containing the IRES-00 or the IRES-01 between CAT and luciferase and, when indicated, the 3′UTR upstream of the poly(A) tract of FMDV A/Arg/00 or A/Arg/01 (3′.00 and 3′.01, respectively) were transfected into BHK-21 infected cells. IRES activity was calculated as the luciferase/CAT activity in each extract, relative to that observed in the constructs lacking the 3′UTR. $^{**}p < 0.01$; ns: not significant. All the results are representative of three experiments. T7: T7 RNA polymerase promoter; Tt: transcription termination signals.

In vivo IRES-dependent translation activity

Bicistronic plasmids carrying the FMDV IRES between the chloramphenicol acetyltransferase (CAT) and luciferase (Luc) genes and, when indicated, the FMDV 3′ end sequences downstream of the second cistron were constructed using plasmids pBIC (Martínez-Salas et al., 1993) and pBIC-3′NCR (López de Quinto et al., 2002). FMDV A/Arg/00 IRES (IRES-00) and FMDV A/Arg/01 IRES (IRES-01) were amplified from plasmids pQ-IRES.00 and pA2001c, respectively, with primers IRESs (5′–CCGAGCTCTGCAGGTTTCCCCAACCG-3′) and IRESa (5′–ATAGAGCTCAAAATCAGTGAGTATAAAGG-3′). The purified products were digested with *Sac*I and ligated to pBIC and pBIC-3′NCR, similarly treated, generating the constructs pIRES-00/Luc, pIRES-01/Luc, pIRES-00-3′NCR and pIRES-01-3′NCR. The region of the 3′UTR previous to the poly(A) tract of FMDV A/Arg/00 (3′.00) and FMDV A/Arg/01 (3′.01) was amplified by PCR. The 3′.00 region was amplified from A/Arg/00 cDNA with primers 3utrAvrF (5′- ACCTAGGTCCCTCAGAGATCACGAT-3′) and 3utrNotR.00 (5′- AGCGGCCGCGGAATTAGGAAGCGGGAA-3′). The 3′.01 region was amplified from plasmid pA2001c with primers 3utrAvrF and 3utrNotR.01 (5′–AGCGGCCGCTGAAATAGGAAGCGGGAA-3′). The PCR fragments and the plasmids pIRES.00-3′NCR and pIRES.01-3′NCR were digested with *Avr*II and *Not*I. The constructs pIRES-00/3′.00, pIRES-00/3′.01, pIRES-01/3′.00 and pIRES-01/3′.01 were generated by ligation of each digested PCR fragment to both plasmids.

Bicistronic plasmids pIRES-00/Luc, pIRES-01/Luc, pIRES-00/3′.00, pIRES-00/3′.01, pIRES-01/3′.00 and pIRES-01/3′.01 were assayed in BHK-21 cells. Transfection of 80–90% confluent monolayers was carried out using Lipofectamine (Gibco-BRL/Invitrogen, Carlsbad, *CA*, USA) 1 hpi with the vaccinia virus VTF7-3 expressing T7 RNA polymerase (Fuerst et al., 1986). Extracts from 2×10^6 cells were prepared at 20 h post transfection (hpt) in 200 μl of Reporter Lysis Buffer (Promega, Madison, WI, USA). The activity of the CAT reporter gene was quantified by a CAT Enzyme Assay System (Promega, Madison, WI, USA) following the manufacturer's protocol. The activity of the Luc reporter gene was quantified using the Luciferase Assay System (Promega, Madison, WI, USA) in a Veritas luminometer (Turner Biosystems Inc., Sunnyvale, CA, USA). The values obtained from the Luc assays were normalized against activity scored from the CAT assay. The adjusted relative light units (RLUs) were plotted using GraphPad Prism 5.0 (GraphPad Software, San Diego, CA, USA). Experiments were performed on triplicate wells and each experiment was repeated at least three times.

hSHAPE analysis

Plasmids pIRES-00/Luc and pIRES-01/Luc were digested with *Pst*I; the CAT gene was excised and plasmids were religated to obtain the constructs pT7-IRES.00 and pT7-IRES.01. These constructs were *Not*I-linearized and *in vitro* transcribed as described above.

Treatment of samples for hSHAPE analysis was performed essentially as described by McGinnis et al. (2009). Briefly, 2 pmol RNA were folded *in vitro* at 37 °C in folding buffer (HEPES 100 mM pH 8, $MgCl_2$ 6 mM, NaCl 100 mM) and treated with N-methylisatoic anhydride (NMIA, (+) reagent reaction) or dimethylsulfoxide (DMSO, (−) reagent reaction). For primer extension, equal amounts of (+) or (−) reactions were incubated with 2 pmol of either 5′ VIC or FAM-labeled pBIC antisense primer (5′–GGCCTTTCTTTATGTTTTTGGCG-3′). Similarly, two sequencing reactions were performed with *in vitro* folded non-treated RNA and fluorescently labeled pBIC antisense primer. Extension was conducted in a final volume of 25 μl containing reverse transcriptase (RT) buffer, 0.6 mM of each dNTP and 100 U of Superscript III RT

(Invitrogen, Carlsbad, CA, USA). In turn, sequencing reactions also included one ddNTP each. cDNA products present in (+) and (−) reactions were combined with sequencing reactions and recovered by ethanol precipitation followed by electrophoresis separation on a 50-cm capillary using a 3130xl Genetic Analyzer (Applied Biosystems). The 3130 POP-7™ polymer was used on the 3130xl System as the separation matrix. For SHAPE data processing, the intensities of the reactive nucleotides were quantified with SHAPEfinder software (Vasa et al., 2008). The average reactivity at each position from two separate SHAPE analyses was incorporated into the RNAstructure software (version 5.3, Mathews Lab) and final RNA structures were generated using RnaViz software (De Rijk et al., 2003).

Acknowledgments

This work was supported by grants PICT035-PAE 37206 from Agencia Nacional de Promoción Científica y Tecnológica and FMD Project AESA-201721 from Instituto Nacional de Tecnología Agropecuaria (Argentina), and BFU2011-25437 from MINECO (Spain). M.I.G., G.K., A.B., O.T. and E.C. are members of the National Research Council (CONICET) Research Career Program. We thank Osvaldo Zábal, Juan Manuel Schammas and Gastón Zábal for technical assistance during our work in the BSL-3A facilities at the CICVyA-INTA, and Noemí Fernández for invaluable support with SHAPE experiments.

Appendix A. Supporting information

Supplementary data associated with this article can be found in the online version at http://dx.doi.org/10.1016/j.virol.2013.10.027.

References

Belsham, G.J., 2009. Divergent picornavirus IRES elements. Virus Res. 139, 183–192.
Carrillo, C., Tulman, E.R., Delhon, G., Lu, Z., Carreno, A., Vagnozzi, A., Kutish, G.F., Rock, D.L., 2005. Comparative genomics of foot-and-mouth disease virus. J. Virol. 79, 6487–6504.
Clarke, B.E., Brown, A.L., Currey, K.M., Newton, S.E., Rowlands, D.J., Carroll, A.R., 1987. Potential secondary and tertiary structure in the genomic RNA of foot and mouth disease virus. Nucleic Acids Res. 15, 7067–7079.
De Rijk, P., Wuyts, J., De Wachter, R., 2003. RnaViz 2: an improved representation of RNA secondary structure. Bioinformatics 19, 299–300.
Domingo, E., Escarmís, C., Baranowski, E., Ruiz-Jarabo, C.M., Carrillo, E., Nuñez, J.I., Sobrino, F., 2003. Evolution of foot-and-mouth disease virus. Virus Res. 91, 47–63.
Donaldson, A., 2004. Clinical signs of foot-and-mouth disease. In: Sobrino, F., Domingo, E. (Eds.), In Foot and Mouth Disease: Current Perspectives. Horizon Bioscience, Norfolk, Inglaterra, pp. 93–102.
Escarmís, C., Toja, M., Medina, M., Domingo, E., 1992. Modifications of the 5′ untranslated region of foot-and-mouth disease virus after prolonged persistence in cell culture. Virus Res. 26, 113–125.
Falk, M.M., Sobrino, F., Beck, E., 1992. VPg gene amplification correlates with infective particle formation in foot-and-mouth disease virus. J. Virol. 66, 2251–2260.
Fernández-Miragall, O., Martínez-Salas, E., 2003. Structural organization of a viral IRES depends on the integrity of the GNRA motif. RNA 9, 1333–1344.
Fernández-Miragall, O., Martínez-Salas, E., 2007. In vivo footprint of a picornavirus internal ribosome entry site reveals differences in accessibility to specific RNA structural elements. J. Gen. Virol. 88, 3053–3062.
Fernández-Miragall, O., Ramos, R., Ramajo, J., Martínez-Salas, E., 2006. Evidence of reciprocal tertiary interactions between conserved motifs involved in organizing RNA structure essential for internal initiation of translation. RNA 12, 223–234.
Fernández, N., Buddrus, L., Piñeiro, D., Martínez-Salas, E., 2013. Evolutionary conserved motifs constrain the RNA structure organization of picornavirus IRES. FEBS Lett. 587, 1353–1358.
Fernández, N., Fernández-Miragall, O., Ramajo, J., García-Sacristán, A., Bellora, N., Eyras, E., Briones, C., Martínez-Salas, E., 2011. Structural basis for the biological relevance of the invariant apical stem in IRES-mediated translation. Nucleic Acids Res. 39, 8572–8585.
Fuerst, T.R., Niles, E.G., Studier, F., Moss, B., 1986. Eukaryotic transient-expression system based on recombinant vaccinia virus that synthesizes bacteriophage T7 RNA polymerase. Proc. Nat. Acad. Sci. U.S.A. 83, 8122–8126.
García-Nuñez, S., König, G., Berinstein, A., Carrillo, E., 2010. Differences in the virulence of two strains of Foot-and-Mouth Disease Virus Serotype A with the same spatiotemporal distribution. Virus Res. 147, 149–152.
Gharbi, J., el Hiar, R., Ben M'hadheb, M., Jaidane, H., Bouslama, L., N'Saibia, S., Aouni, M., 2006. Nucleotide sequences of IRES domains IV and V of natural ECHO virus type 11 isolates with different replicative capacity phenotypes. Virus Genes 32, 269–276.
Gromeier, M., Alexander, L., Wimmer, E., 1996. Internal ribosomal entry site substitution eliminates neurovirulence in intergeneric poliovirus recombinants. Proc. Nat. Acad. Sci. U.S.A. 93, 2370–2375.
Grubman, M.J., Baxt, B., 2004. Foot-and-mouth disease. Clin. Microbiol. Rev. 17, 465–493.
Jackson, T., King, A.M., Stuart, D.I., Fry, E., 2003. Structure and receptor binding. Virus Res. 91, 33–46.
Knowles, N.J., Samuel, A.R., 2003. Molecular epidemiology of foot-and-mouth disease virus. Virus Res. 91, 65–80.
Kuhn, R., Luz, N., Beck, E., 1990. Functional analysis of the internal translation initiation site of foot-and-mouth disease virus. J. Virol. 64, 4625–4631.
Li, R., Zou, Q., Chen, L., Zhang, H., Wang, Y., 2011. Molecular analysis of virulent determinants of enterovirus 71. PLoS One 6, e26237.
López de Quinto, S., Martínez-Salas, E., 1997. Conserved structural motifs located in distal loops of aphthovirus internal ribosome entry site domain 3 are required for internal initiation of translation. J. Virol. 71, 4171–4175.
López de Quinto, S., Martínez-Salas, E., 2000. Interaction of the eIF4G initiation factor with the aphthovirus IRES is essential for internal translation initiation *in vivo*. RNA 6, 1380–1392.
López de Quinto, S., Sáiz, M., de la Morena, D., Sobrino, F., Martínez-Salas, E., 2002. IRES-driven translation is stimulated separately by the FMDV 3′-NCR and poly (A) sequences. Nucleic Acids Res. 30, 4398–4405.
Lowe, P.A., Brown, F., 1981. Isolation of a soluble and template-dependent foot-and-mouth disease virus RNA polymerase. Virology 111, 23–32.
Mackiewicz, V., Cammas, A., Desbois, D., Marchadier, E., Pierredon, S., Beaulieux, F., Dussaix, E., Vagner, S., Roque-Afonso, A.M., 2010. Nucleotide variability and translation efficiency of the 5′ untranslated region of hepatitis A virus: update from clinical isolates associated with mild and severe hepatitis. J Virol. 84, 10139–10147.
Martínez-Salas, E., 2008. The impact of RNA structure on picornavirus IRES activity. Trends Microbiol. 16, 230–237.
Martínez-Salas, E., Ryan, M., 2010. Genome replication and translation. In: Ehrenfeld, E., Domingo, E., Roos, R. (Eds.), The Picornaviruses. ASM Press, Washington DC.
Martínez-Salas, E., Sáiz, J.C., Dávila, M., Belsham, G.J., Domingo, E., 1993. A single nucleotide substitution in the internal ribosome entry site of foot-and-mouth disease virus leads to enhanced cap-independent translation *in vivo*. J Virol. 67, 3748–3755.
Martínez, M.A., Carrillo, C., Plana, J., Mascarella, R., Bergada, J., Palma, E.L., Domingo, E., Sobrino, F., 1988. Genetic and immunogenic variations among closely related isolates of foot-and-mouth disease virus. Gene 62, 75–84.
Mason, P.W., Bezborodova, S.V., Henry, T.M., 2002. Identification and characterization of a cis-acting replication element (cre) adjacent to the internal ribosome entry site of foot-and-mouth disease virus. J. Virol. 76, 9686–9694.
Mason, P.W., Grubman, M.J., Baxt, B., 2003. Molecular basis of pathogenesis of FMDV. Virus Res. 91, 9–32.
Mattion, N., König, G., Seki, C., Smitsaart, E., Maradei, E., Robiolo, B., Duffy, S., Leon, E., Piccone, M., Sadir, A., et al., 2004. Reintroduction of foot-and-mouth disease in Argentina: characterisation of the isolates and development of tools for the control and eradication of the disease. Vaccine 22, 4149–4162.
McGinnis, J.L., Duncan, C.D., Weeks, K.M., 2009. High-throughput SHAPE and hydroxyl radical analysis of RNA structure and ribonucleoprotein assembly. Methods Enzymol. 468, 67–89.
Medina, M., Domingo, E., Brangwyn, J.K., Belsham, G.J., 1993. The two species of the foot-and-mouth disease virus leader protein, expressed individually, exhibit the same activities. Virology 194, 355–359.
Moffat, K., Howell, G., Knox, C., Belsham, G.J., Monaghan, P., Ryan, M.D., Wileman, T., 2005. Effects of foot-and-mouth disease virus nonstructural proteins on the structure and function of the early secretory pathway: 2BC but not 3A blocks endoplasmic reticulum-to-Golgi transport. J Virol. 79, 4382–4395.
O'Donnell, V.K., Pacheco, J.M., Henry, T.M., Mason, P.W., 2001. Subcellular distribution of the foot-and-mouth disease virus 3A protein in cells infected with viruses encoding wild-type and bovine-attenuated forms of 3A. Virology 287, 151–162.
Ramos, R., Martinez-Salas, E., 1999. Long-range RNA interactions between structural domains of the aphthovirus internal ribosome entry site (IRES). RNA 5, 1374–1383.
Rieder, E., Bunch, T., Brown, F., Mason, P.W., 1993. Genetically engineered foot-and-mouth disease viruses with poly(C) tracts of two nucleotides are virulent in mice. J. Virol. 67, 5139–5145.
Roberts, L.O., Seamons, R.A., Belsham, G.J., 1998. Recognition of picornavirus internal ribosome entry sites within cells; influence of cellular and viral proteins. RNA 4, 520–529.
Rueckert, R.R., 2001. Picornaviridae: the viruses and their replication, In Fields virology. In: Knipe, D., Howley, P., Griffin, D., Lamb, R., Martin, M., Roizman, B., Straus, S. (Eds.), Lippincott-Raven, Philadelphia, PA, USA, pp. 609–654.
Rueckert, R.R., Wimmer, E., 1984. Systematic nomenclature of picornavirus proteins. J Virol. 50, 957–959.
Sáiz, M., Gómez, S., Martínez-Salas, E., Sobrino, F., 2001. Deletion or substitution of the aphthovirus 3′ NCR abrogates infectivity and virus replication. J Gen. Virol. 82, 93–101.

Sangar, D.V., Rowlands, D.J., Harris, T.J., Brown, F., 1977. Protein covalently linked to foot-and-mouth disease virus RNA. Nature 268, 648–650.
Serrano, P., Pulido, M.R., Sáiz, M., Martínez-Salas, E., 2006. The 3′ end of the foot-and-mouth disease virus genome establishes two distinct long-range RNA–RNA interactions with the 5′ end region. J. Gen. Virol. 87, 3013–3022.
Sobrino, F., Domingo, E., 2004. Foot and Mouth Disease: Current Perspectives. Horizon Bioscience, Norfolk, United Kingdom.
Van Rensburg, H.G., Mason, P.W., 2002. Construction and evaluation of a recombinant foot-and-mouth disease virus: implications for inactivated vaccine production. Ann. N.Y. Acad. Sci. 969, 83–87.
Vasa, S.M., Guex, N., Wilkinson, K.A., Weeks, K.M., Giddings, M.C., 2008. ShapeFinder: a software system for high-throughput quantitative analysis of nucleic acid reactivity information resolved by capillary electrophoresis. RNA 14, 1979–1990.